SPE-174194-MS

Understanding Perforation Geometry Influence on Flow Performance Using CFD

Simon Allison, Delphian Ballistics Limited; Dr. Jörn Löhken, and Liam Mc Nelis, DynaEnergetics;
Dr. Lesmana Djayapertapa, Michael Byrne, and Ken Watson, LR Senergy; Alistair Clarke, Premier Oil Limited

This paper was prepared for presentation at the SPE European Formation Damage Conference and Exhibition held in Budapest, Hungary, 3–5 June 2015.

Abstract

Perforations are required to establish effective hydraulic communication between the wellbore and the surrounding formation. An often considered key attribute is to achieve maximum penetration, providing an effective flow path by extending through the near-wellbore damaged region, penetrating undamaged reservoir beyond.

The challenge is always to design the perforation system to maximise flow efficiency. In the majority of instances deeper penetration is a key design parameter, but penetration is affected not only by the shaped charge, but also critically by rock strength and stress effects. Therefore, perhaps of greater importance are perforations that are both clean and less damaged, providing a more effective connection to the reservoir, whilst maintaining maximum penetration.

Much has been done to enhance perforation efficiency through the development of dynamic underbalance systems and, where appropriate, the application of reactive charge technology. However, little has been done to explore possible benefits resulting from significant changes in perforation geometry, beyond conventional premium system design.

This paper provides a detailed insight into a comprehensive research and development study, following the conclusions obtained for a new convergent perforation system. The system is optimised through harnessed shock-wave energy, achieved by focusing charge groups at a fixed point within the reservoir.

A rigorous section IV test programme was conducted to evaluate the potential flow performance enhancement for such a perforation system. Lab results highlighted a >15% increase in the tested productivity ratio, compared directly to standard system shots, executed under identical conditions.

API-19b Section IV test data validation was carried out using Computation Fluid Dynamics (CFD). A key objective was to match the lab flow performance data, replicating boundary conditions and perforation geometry within each model. CFD modelling enabled further detailed assessment of key relevant parameters influencing improved flow performance, i.e. crushed zone damage and improved channel geometry effects.

Furthermore, CFD was used effectively to model a series of short radial well models, using each matched perforation geometry, comparing the convergent perforation system against the standard HSD

system. These models provided further evaluation of key performance influencing factors such as shot arrangement and phasing effects.

In conclusion, the study has shown, through various levels of verification, adopting a convergent perforation approach to gun system design, can enhance perforation flow efficiency through geometry improvement. CFD modelling also showing, within a radial wellbore arrangement, such a system is capable of improving flow performance by as much as 50%.

Introduction

Well perforations are created principally to establish connection to the reservoir through the cased wellbore. A clean and effective communication path is crucial to optimizing oil / gas production, as well as injection. It has long since been recognized that perforation flow efficiency is directly influenced by the general "skin" components, such as crushed zone (k_c) and the effective perforation penetration length (L_{eff}). However, it is also important to understand what influence perforation geometry can have towards improved flow efficiency, potentially improving well flow performance.

In the vast majority of cases, perforation design sets out to achieve the optimal wellbore connection to the reservoir. Most conventional perforation systems set out to achieve this in the same way, by creating a High Shot Density (HSD) shot pattern, formed radially around the wellbore, delivering a radially phased cluster of perforations in a helical (spiral) form.

Perforation design typically considers three main factors for optimization. These are; shaped charge type, shot density and shot phasing. Concerning shaped charge selection, there are a variety of options available depending on the required application. However, for the majority of production / injection well applications, deep penetrating (DP) charges have become the standard. As the name suggests, DP charges are designed to increase the connected reach from the wellbore, increasing the effective wellbore radius, and ideally penetrating beyond any near wellbore damage, typically sustained during the drilling and completion phases.

The penetration performance of the DP shaped charge has a much to do with the design of the shaped charge. Key design features, such as charge geometry, charge liner design and materials used within the charge itself, combine to play a significant role in charge performance. One additional key factor relates to the type and quantity of explosive being used. In general terms, the penetration achieved from the DP charge is relative to its physical size and design.

The majority of HSD gun systems, used for production well applications, are designed to maximize both penetration and shot density. Shot density becomes directly related to charge size. The larger the charge typically means a reduction in the shot density, defined as the number of shots (perforations) per unit length of gun. For example, depending on the selected charge size, the conventional HSD gun would typically have 6 shots/ft for the majority gun systems, using the optimal size of charge to achieve maximum penetration.

HSD gun systems look to achieve an even radial separation between shots, where radial coverage can be exploited to improve flow. The majority of conventional systems designed to achieve full radial coverage within a 1-ft unit interval, i.e. a six shots per foot (6 shots/ft) having 60° equal phasing, providing 360° radial coverage per foot.

Standard HSD perforation system design follows a convention that penetration, shot density and phasing are all directly linked, each impacting the next in the final design & construction of the gun. Perforation damage, sustained as a result of grain crushing (k_c) and channel debris plugging, having a serious effect on flow performance. Removal of this damage is typically achieved using underbalance, either through static (SUB) and/or dynamic (DUB) under-balancing.

SUB is where the well is placed at a "targeted" lower pressure below reservoir / pore pressure prior to perforating. SUB can only be achieved when the well is 'unperforated' or the reservoir has been pressure isolated. Lowering the well pressure below pore pressure results in a sudden influx of reservoir fluid

through the newly created perforations. The resulting flow acts to remove as much of the crushed grain and debris plugged perforation damage as is possible.

DUB is a naturally occurring pressure phenomena created through the sudden influx of well wellbore fluids into the guns outer hollow carrier. The hollow carrier gun is a sealed atmospheric chamber, once detonated, opens the chamber immediately to wellbore fluid. This results in a sudden vacuum effect, pulling wellbore fluids into the carrier chamber, reducing the surrounding pressure by 1000's psi, sustained over a period of a few seconds only. Such effects are well documented, and through opimisation, DUB has been shown to offer a significant benefit towards perforation damage removal.

Evaluation of perforation geometry, as a true performance factor, requires consideration towards an altogether different gun design. As a result, this paper sets out to understand the effect of geometry optimization, achieved through a unique, converging, charge arrangement. Designed using groups of three shaped charges, the converging charges are focused on a single point in the formation. The result is a focused area of energy displacement within the convergent region, pulverizing the rock as opposed to crushing, resulting in a larger, less damaged, combined perforation channel.

The research objective was to establish a laboratory test program, to help understand and evaluate the flow efficiency effect for such a design, when compared to standard systems. To do so, an extensive, modified, API section IV program was devised. Further to this, computational fluid dynamics (CFD) was used to provide a full performance evaluation of each tested perforation through matching the lab data. CFD was again used to create short radial well models, simulating the phasing & relative shot density effects associated with convergent perforation vs standard HSD system.

The work programme stages undertaken have been outlined as follows:

I. API Section IV Test Programme – Performance evaluation of convergent & conventional perforations

   a. Phase 1 – Concept Test
   b. Phase 2 – Concept Validation
   c. Phase 3 – Concept Optimistaion

II. Phase 1 CFD simulation – Section IV Test Data Matching:

   a. Model and match standard perforation – Damage and Core Flow Efficiency
   b. Model and match convergent perforation – Damage and Core Flow Efficiency

III. Phase 2 CFD Simulation – Radial wellbore model for performance comparison of each perforation system:

   a. Standard HSD phased perforation system using matched perforation performance models
   b. Convergent phased perforation system using matched perforation performance models

API Section IV Test Programme Description

Flow laboratories of this type have been used for extensively for the evaluation of perforation performance under simulated downhole pressure conditions. For this purpose, the test programme was designed to enable a fair and comprehensive comparison between convergent and standard perforation performance, under a consistent set of simulated downhole conditions.

Standard API Section IV test equipment is designed principally for performance testing of single charges. Testing the convergent perforation system requires inclusion of a grouped shaped charge arrangement into the charge chamber. For this test programme groups of three charges were used (figure 1), appropriately sized to fit safely within the charge chamber.

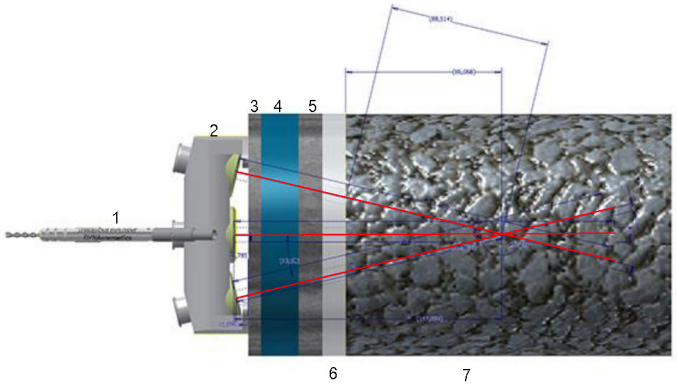

Item Description:

1. Detonator
2. Moulded shaped charge holder
3. Hollow carrier steel plate
4. Water filled void – gun stand-off
5. Wellbore casing plate
6. Annular cement
7. Test Core

Figure 1—Convergent Perfoation Section IV Test Set-up

All testing was conducted in accordance with standard API Section IV test protocols. Each core prepared in the same way, first oven dried, measured and weighed prior to fluid saturation. All cores were of a consistent geological type and dimension:

- Sander Schlf – Core dimension 7″ dia × 15″ long
- UCS – 6000 to 8000 psi
- Porosity – 19 to 22%

Flow media used was Odorless Mineral Spirit (OMS). Once saturated, the core was weighed and vacuum saturated, fluid volume was measured to calculate the respective core porosity and bulk density values. Each core is then inserted into a rubber sleeve prior to being placed into the test chamber, figure 2. The rubber sleeve provides pressure isolation between the applied overburden pressure, used to simulate stress, and the pore pressure. Pore pressure is applied via the flow inlet (distributor), with wellbore pressure independently set to simulate static underbalance condition. Figure 2, highlights the test set-up conditions applied in the test programme.

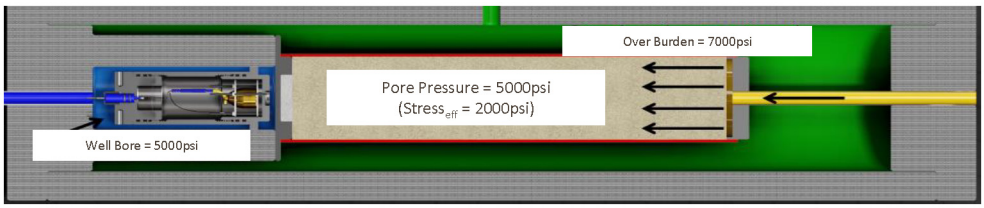

Figure 2—Section IV Test Conditions

Three test procedures were used for performance evaluation and comparison of convergent and standard test:

- Three charge – convergent [A]
- Single charge – standard [B]
- Three charge – standard [C]

Each test design is illustrated in figure 3, executed using the same test protocol, following identical pre & post-perforation flow routines. Figure 3 also illustrates that each “pre-flow” is conducted using a drilled casing plate, used to simulate the post-perforation casing plate condition. i.e. a ‘single’ drilled hole casing plate for a single perforation test [Type B], and a ‘three’ hole casing plate used for both standard and convergent tests [Type A & C]. The core is exposed to both a pre & post perforation flow, with flow entering the core through a flow distributor, providing full radial flow coverage, flowing in an axial path

to the output point (wellbore). The relevance of the casing plate used in the pre-flow is to ensure the same flow convergence effects and boundary conditions are represented and assessed in both pre & post perforation flow periods for accurate determination of the productivity ratio (PR).

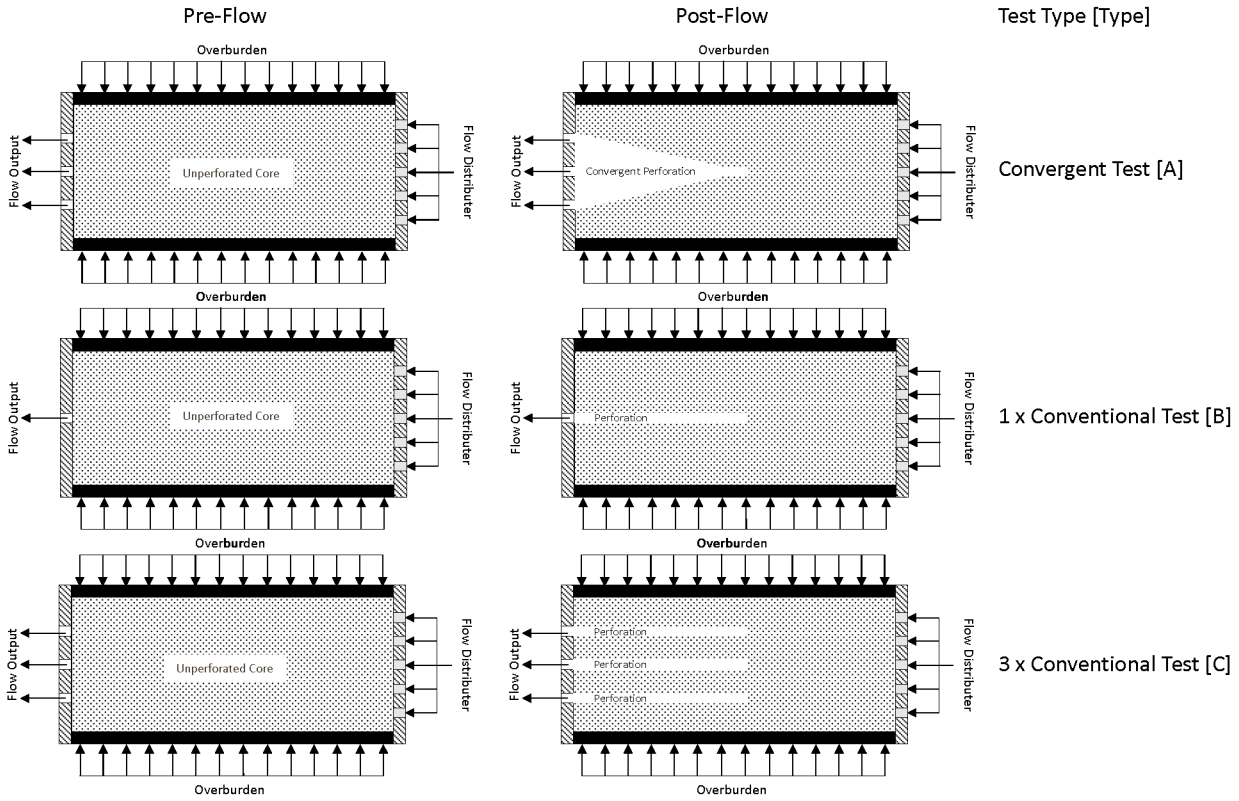

Figure 3—API Section IV Test Programme Design

For each test the wellbore chamber was set on balance to pore pressure, meaning no static underbalance (SUB) was applied. Therefore, each shot relying solely on the dynamic underbalance (DUB) effects to achieve a consistent set of perforation clean-up parameters. Figure 5, highlights the DUB effect from a selection of the test types.

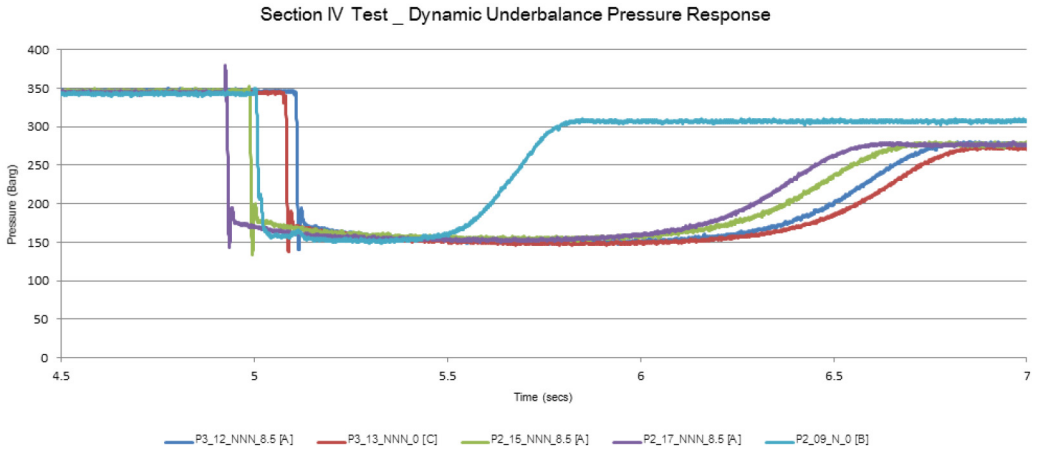

Figure 5—Section IV Test DUB Data Plot

Figure 5 illustrates the DUB transient effect from the perforation event, showing a near identical instantaneous drop in wellbore pressure of approx. 200barg (2900psi), resulting from the vacuum effect created by sudden exposure of the atmospheric pressured charge chamber to wellbore pressure. All shots executed with a three charge configuration, types A & C, exhibit near identical DUB period, which is considerably extended compared to the single shot (type B). This effect is due to the increase in "free volume" created by detonation of three charges vs. the single, taking slightly longer for fluids to fill the void created.

The primary test objective is to acquire a series of stabilized pressure & flow measurements to derive the productivity ratio (PR) for each shot. Each test being conducted over a series of five differential pressures (Δp) stages, each stage at an identical Δp for both pre & post perforation flow (figure 6). The derived PR values become the primary performance evaluation measure, used for shot performance characterization at this stage.

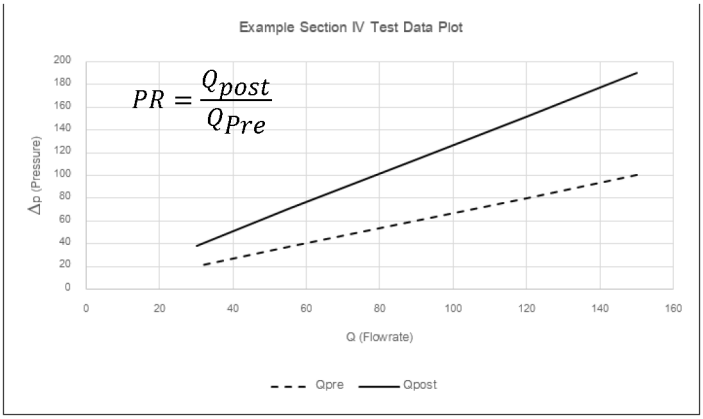

Figure 6—Section IV Test Data Plot (Pre & Post Perforation)

API Section IV Test Programme Results

The test programme, for the comparison of the convergent charge design, was conducted over three phases, these are:

- Phase 1 – Concept Test
- Phase 2 – Concept Validation
- Phase 3 – Concept Optimistaion

Phase 1, concept test, was executed primarily to establish the optimal test design set-up, rock type selection, test fluid selection, optimal charge sizes etc. Phase 2, concept validation, being the main data acquisition phase, where repeated testing was conducted to fully appraise the PR data results, comparing the resulting data distributions for each test type, convergent or standard, Figure 7. In total, more than 35 test shots have been carried out.

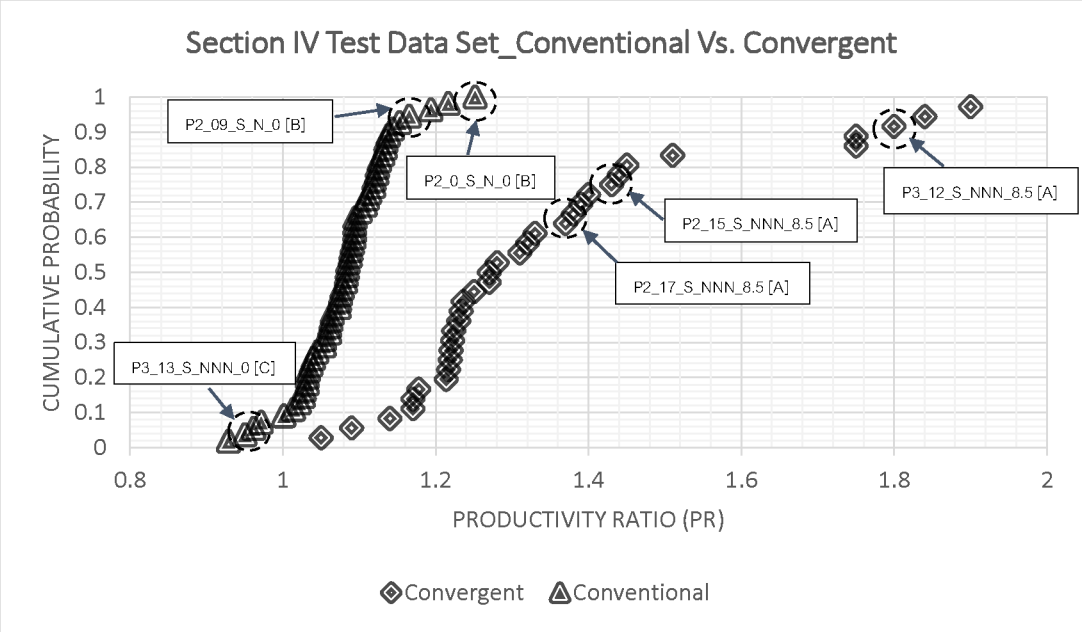

Figure 7—Cumulative Probability PR Test Data – Conventional Vs Converging

Phase 2 testing was conducted using a 'solid' plastic charge module, figure 1. The solid module provided rapid turnaround for charge angle design optimization. However, during testing it became evident that the solid module was responsible for charge interference effects, due to a lateral shockwave transfer between charges through its solid mass. This interference effect presented issues with the resulting convergence pattern, leading to suboptimal geometries.

Phase 3, adopted a new charge module design, replaced by a more sophisticated, precision cut steel charge tube. The charge tube design, representative of the field gun, removed almost all solid mass between the charges, eliminating charge interference, leading to consistency with the convergent shot geometry, resulting in improved PR performance values.

Figures 7 & 8, below, shows the collective PR data distribution acquired from test phases 2 & 3, for both standard [B&C] and convergent [A] tests. Each test using the same charges, these were hand-made 6.5g HMX/St, DP2 from DynaEnergetics.

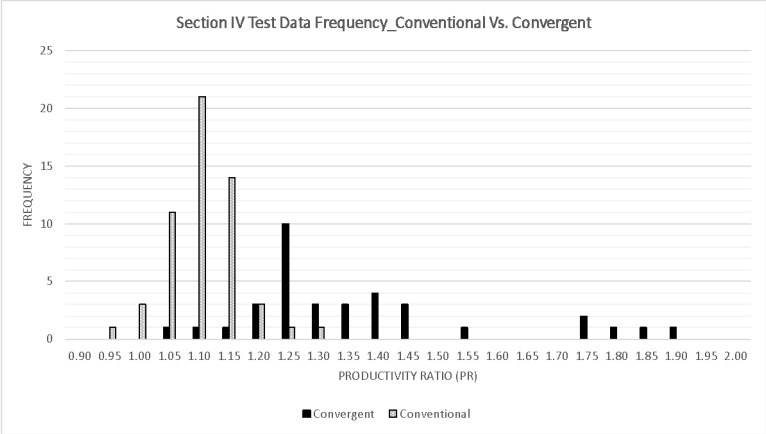

Figure 8—Test Data PR Distribution – Conventional Vs. Convergent

The PR data presented in figures 7 & 8 highlight the improved individual perforation flow performance gained by the convergent charge set-up. Direct comparison of the 'mean' values show the convergent set-up has an increased PR of circa. 30%. Comparisons to the 'maximum' highlights further potential improvement of circa. 50%. The data shows the convergent set-up achieving a low PR value of 1.05, which closely approximates to the standard (conventional) set-up 'mean' value (1.08). The convergent system also showing a mean case that is circa. 10% improved on the standard systems 'high' value, further highlighting the minimal downside performance risk for the convergent perforation set-up.

Six tests, summarized in table 2, were selected for CFD simulation. These tests selected given their PR values were strongly representative of the overall range for each test set-up. All six were analysed using CFD, to assess the influence perforation geometry has on overall flow performance.

Table 1—PR Test Data Distribution Summary

Data Distribution	Convergent	Conventional
Mean	1.38	1.08
Range	0.85	0.44
Minimum	1.05	0.81
Maximum	1.90	1.25

Table 2—Selected API Section IV Test Data Summary.

Test ID	Test Phase	Charge Set-Up	Test Type	Module	Charges	Perm (md)	PR
P2_00_S_N_0	2	Standard	B	Solid	Single	310.0	1.22
P2_09_S_N_0	2	Standard	B	Solid	Single	694.0	1.18
P3_13_S_NNN_0	3	Standard	C	Tube	Three	45.9	0.81
P2_15_S_NNN_8.5	2	Convergent	A	Solid	Three	162.0	1.44
P2_17_S_NNN_8.5	2	Convergent	A	Solid	Three	288.0	1.38
P3_12_S_NNN_8.5	3	Convergent	A	Tube	Three	11.61	1.81

Perforation Geometry Characterization

3D perforation channel geometry models were created using both CT scanned geometry and physical measurement of the perforation channel from core sections.

When tackling CFD modelling and simulation, there are several items that are required during the course of this work, each combining to provide a satisfactory, and accurate, result. One of the first "building blocks" in the process is getting correct geometry, or at least closely representative to the system being investigated. Essentially, a more precise geometry captured in the physical model leads to a more accurate final result.

Given the inevitable geometric irregularities, present in the actual perforation geometry, it was necessary to 'clean up' the perforation shapes, providing symmetry to simplify model construction. Improtantly this is done whilst remaining true to the measured surface area and channel volumes, from those extracted from the original measured and scanned shapes.

As previously mentioned, the charge interference from the solid module design caused irregularities with the convergent channel shape. As shown in table 3, the geometry in this case was not fully converged, or non-ideal, therefore a similar, partially converged perforation geometry was created to represent test of this type. The non-ideal nature of the channel was better revealed on CT scans, showing a less complete communication across all three converging perforation channels. This perforation geometry is referred to as "TriDent", where the other geometry models are referred to as "TriStim" and "Standard".

Table 3—Perforation Geometry Model Characterization

Geometry - Standard	Geometry - TriStim (Convergent)	Geometry - TriDent (Convergent)
		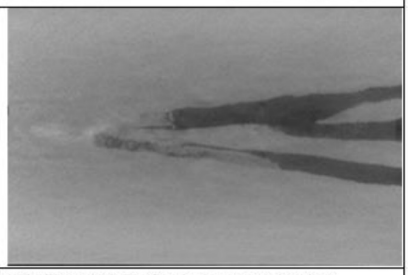
Conv. 3D Geometry Model	"TriStim" 3D Geometry Model	"TriDent"3D Geometry Model
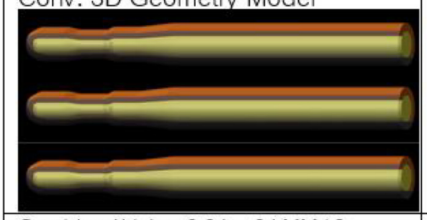	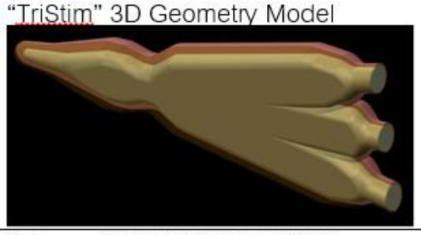	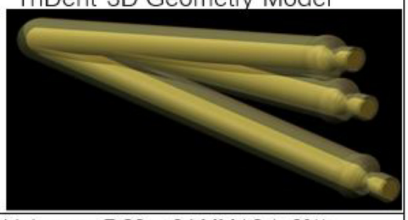
Combined Vol. = 6.84e+04 MM^3 Combined Surf. Area = 2.3e+04 MM^2	Volume = 1.30e+05 MM^3 (+90%) Surface Area = 2.52e+04 MM^2 (+10%)	Volume = 7.23e+04 MM^3 (+6%) Surface Area = 2.14e+04 MM^2 (-7%)
P2_00_S_N_0 (Single) P2_09_S_N_0 (Single) P3_13_S_NNN_0 (Three)	P3_12_S_NNN_8.5 (Three Convergent)	P2_15_S_NNN_8.5 (Three Convergent) P2_17_S_NNN_8.5 (Three Convergent)

Creation of representative CAD 3D perforation models, table 3, enable full characterisation the geometries for "TriStim", "TriDent" and "Standard", each including an outer damaged region, represented by a 5mm thick crushed zone, enabling skin matching for each simulation case.

Creation of the 3D perforation models helped assess the key geometric characteristics between each. Again, summarized in table 3, the standard perforation CAD model has been compared in terms of its surface area and volume. Doing so, revealed the relative 'TriStim' surface area is circa. 10% greater than the comparative standard 'three' perforation geometry model. Similarly, the volume of the TriStim channel increases significantly, by 90%, by direct comparison. Similar comparison of the 'non-ideal' TriDent model shows a reduction in surface area, down circa. 7% by comparison, while the overall channel volume remains slightly increased, by 6%. This highlights one critical benefit associated with achieving a full convergent geometry.

Each geometry model is selected to best represent the relevant tested perforation. The model can then be used to simulate and match the lab core flow performance. The same individual matched perforation models are then scaled for radial well-flow effect analysis. CFD enables relevant comparative perforation features, such as orientation and phasing, to be modelled accurately.

CFD Simulation Modelling

Computational Fluid Dynamics (CFD), in simple terms, is a computational method used to model and simulate fluid flow in bounded domains. The bounded domains, sometimes referred to as Regions, are needed to generate what is known as 'volume mesh' where the fluid would flow. These Regions can be Solid Region, e.g. for heat transfer analysis, Fluid Region, where there are no restrictions, or they can be Porous Region to simulate permeable media such as sandstone reservoir. The fluid simulated could be of any type: liquids (e.g. water, oil), gas (e.g. air, methane), or particles (e.g. sand). The combination of multiple fluids, known as multiphase, can also be simulated, however, in this particular case only single phase simulation was required.

CFD is based on fundamental physics, and the governing equations of fluid flow represent mathematical statements of the conservation laws of physics. In other words, the motion of a fluid element in a three dimensional space is described by:

- The continuity equation (the mass of a fluid is conserved)
- The momentum equation (the rate of change of momentum equals the sum of the forces on a fluid particle); and
- The Energy equation (the rate of change of energy is equal to the sum of the rate of heat addition to and the rate of work done on a fluid particle)

CFD is a powerful technique and a proven technology, particularly in the aerospace and automotive industries; and today it is increasingly being used to model the near wellbore behavior, including modeling and simulation of perforation flow performance under specific test conditions. The use of CFD enables accurate replication of the boundary and flow conditions present during the test, as well as enabling an accurate characterization of the perforation geometry. This bodes very well with one of the aims of this study: to understand what influence perforation geometry can have towards improved flow efficiency.

Lab Test Flow Performance Matching

In each perforation flow experiment, the pre & post perforation PI is determined from the axial stabilized flow response, through the full range of differential pressure stages.

For each model, the stabilized flow response from the 'pre-flow' test is simulated and matched. Each model having been constructed to replicate the core dimension, fluid type, flow convergence and boundary conditions present during the flow test:

- Core dimension as per test 7″ dia × 15″ length,
- Fully distributed Axial flow, shown from left to right,
- Casing plate type: single or three hole
- No flow boundary around outer radius.

Table 4, highlights the model construction used for the various pre-flow simulations, used to derive each core average (undamaged) permeability (k). Permeability being the single variable used to match the output flow response for each staged differential pressure.

Table 4—Pre-flow CFD Model

Single Perforation Pre-Flow – CFD Model	Three Perforation Pre-Flow – CFD Model
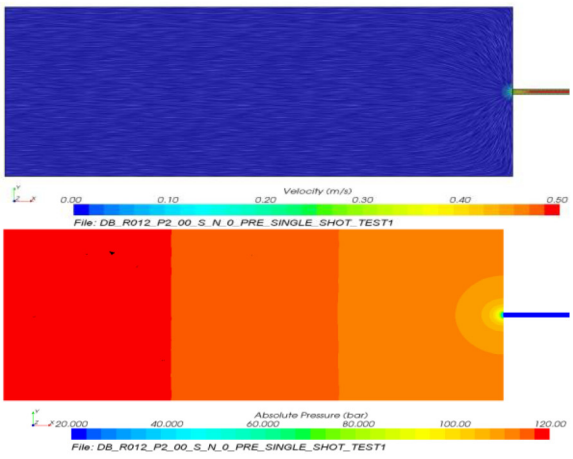	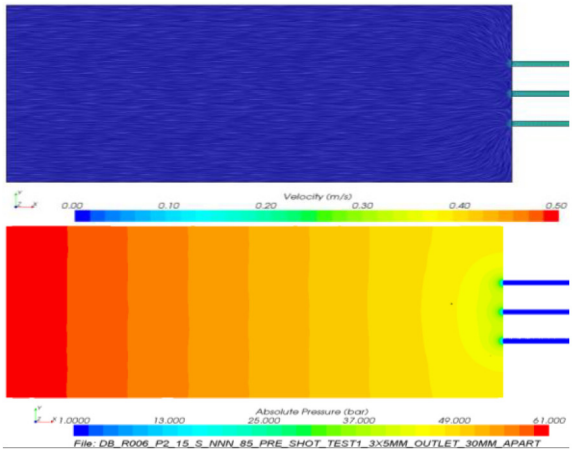
• Flow convergence effect at exit relative to casing plate – Single 5mm Ø exit.	• Flow convergence effect at exit relative to casing plate – Three x 5mm Ø exit.

Figure 9, shows an example of the matched output flow response of the model compared to the measured lab data. In each of the selected tests the core / undamaged permeability (k) has been matched to the tested 'pre-flow' measurments, summarized in table 5.

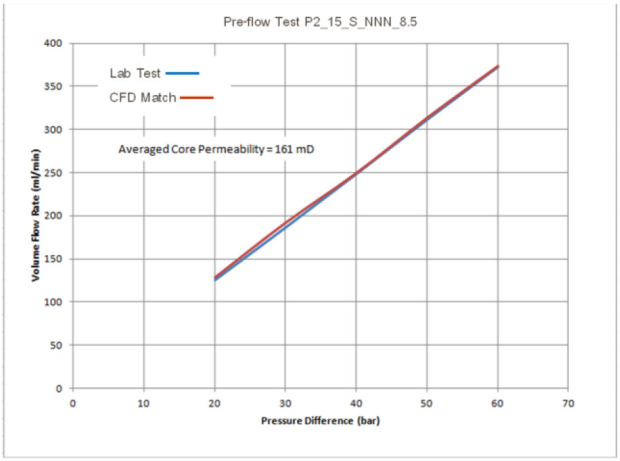

Figure 9—Example CFD 'Pre-Flow' Test Data Match

Table 5—CFD Permeability Pre-Flow Match

Test ID	Test Phase	Casing plate	Derived Perm (md)
P2_00_S_N_0	2	Single	310.0
P2_09_S_N_0	2	Single	694.0
P3_13_S_NNN_0	3	Three	56.0
P2_15_S_NNN_8.5	2	Three	161.0
P2_17_S_NNN_8.5	2	Three	288.0
P3_12_S_NNN_8.5	3	Three	14.3

The same exercise is done for the post perforation flow, where the model is populated with the appropriate perforation geometry, using k_c as the sole tuning variable to match the respective flow response, keeping the assumed crushed thickness (t_c) and effective length (L_{eff}) constant. Examples of the 'post perforation' flow models, and their respective tests, are summarized in table 6.

Table 6—Matched Post Perforation Flow Models

Single Standard Perf Model	Three Standard Perf Model	TriDent Converge Perf Model	TriStim Converge Perf Model
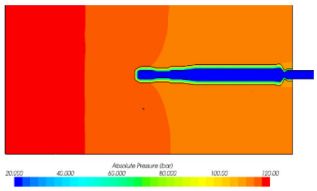	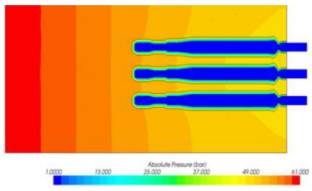	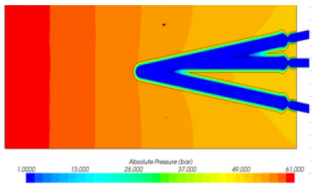	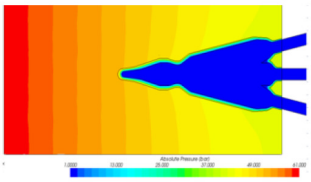
P2_00_S_N_0 P2_09_S_N_0	P3_13_S_NNN_0	P2_15_S_NNN_8.5 P2_17_S_NNN_8.5	P3_12_S_NNN_8.5

The dominant factors influencing perforation skin are the crushed damage (k_c) and the perforation effective length (L_{eff}). It was not possible to accurately characterize the effective length of the perforation from lab tests. Therefore, for consistency, each flow model is matched through manipulation of the crushed damage, k_c, used as a single proxy for 'skin'.

All models were based on a fixed crushed interval thickness, t_c = 0.5cm, with effective length L_{eff} = 100% assumed. The damage ratio, k_c/k is matched to characterize the individual perforation damage, i.e. the relative skin for each case. Figure 10, shows an example output of the post perforation flow match, and table 7, shows the corresponding matched data. The same procedure and output is generated for all six tests.

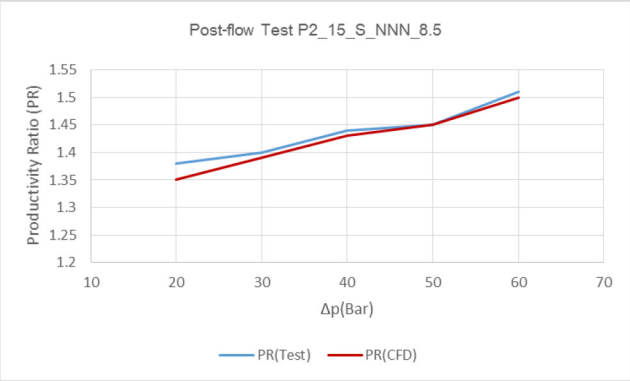

Figure 10—"Post-Flow" matched output PR Values.

Table 7—Test P2_15 Matched Perforation Flow Data.

Test Stage#	Δp(Bar)	Rock Perm (mD)	PR_{Test}	PR_{CFD}	k_c/k (%)	CFE (%)
P2_15 Stage #1	60	161	1.51	1.50	0.56	24.5
P2_15 Stage #2	50	161	1.45	1.45	0.52	23.7
P2_15 Stage #3	40	161	1.44	1.43	0.51	23.4
P2_15 Stage #4	30	161	1.40	1.39	0.53	23.1
P2_15 Stage #5	20	161	1.38	1.35	0.48	22.6
Averaged Data	PR Match = +/- 1.5%		1.44	1.42	0.52	23.5

The matched results, for all tests, are summarized in table 8, showing the matched k_c/k values, along with model match accuracy. Overall the CFD models are matched to within +/−1.5% of the measure PR, showing that the singular matching approach, using k_c, proving to be robust.

Table 8—Matched Perforation Flow Results

Test ID	Geometry	RP_{Test}	PR_{CFD}	Match (-/+%)	k_c/k (%)	PI_{Actual}	$PI_{Theoretic}$	CFE (%)
P2_00_S_N_0	Std. Single	1.22	1.23	0.82	0.32	0.052	0.636	8.20%
P2_09_S_N_0	Std. Single	1.18	1.17	−0.85	0.30	0.108	1.265	8.50%
P3_13_S_NNN_0	Std. Three	0.81	0.82	1.23	0.32	0.021	0.126	16.6%
P2_15_S_NNN_8.5	TriDent	1.44	1.42	-1.39	0.52	0.062	0.266	23.4%
P2_17_S_NNN_8.5	TriDent	1.38	1.38	0.00	0.50	0.111	0.491	22.7%
P3_12_S_NNN_8.5	TriStim	1.81	1.81	0.00	1.12	0.005	0.014	35.1%

Due to the skin matching process, the results show matched k_c/k values notably well below normal expected levels. This is in part, an artifact of the modelling controls, given it was not possible to accurately account for any L_{eff} reduction. However, the higher levels of damage are also thought to be caused by poorer perforation clean-up, caused by limitations of the axial flow test set-up. Under axial conditions the flow of fluid through the core is more restricted than would be the case under radial conditions. It is believed that this flow restriction limits the effectiveness of the immediate clean-up from the dynamic under-balance, potentially contributing a significant part to the higher skin values observed across all tests.

A further stage in the analysis is the calculation of the core flow efficiency (CFE), where the perforation is modelled in absolution of any 'skin'. CFE is often used to quantify perforation flow performance from Section IV tests, but to do so requires CFD simulation. In simplest form, this is the ratio of the 'actual' flow vs. the undamaged or 'theoretic' flow. Computation of the undamaged flow becomes

a relatively simple exercise, removing the damaged region from the respective perforation geometry model and repeating the flow simulation. Using each 'well-defined' perforation geometry, the calculated 'theoretical' flow gives a robust approximation its 'zero damage' theoretic PI. CFE is calculated using the following basic formula:

$$CFE = PI_{Actual}/PI_{theoretic}$$

A key observation from the matching process is the consistency of the k_c/k ratio for each of the tested geometries. Where the standard charge setup was tested, whether in single or three form alignment, there is good repeatability between the k_c/k ratio required match, averaging at 0.31%, each test matching to within +/−1.5%.

The same appears true for the TriDent geometry, each matching with a k_c/k of circa. 0.51%, again matched to within +/−1.5% of the test data. Although the full convergent effect hasn't been achieved, the results appear to show the overall perforation damage has been reduced significantly, circa. 65% reduction by comparison.

Where full convergence is achieved the result indicates a further significant improvement in the comparative k_c/k ratio. The full convergent shot indicating greater than threefold reduction in perforation damage, compared to the standard system, with a near perfect test match.

The 'single' and 'three' standard perforation test geometries yield almost identical k_c/k ratios, however the PR value for the standard three shot test is approximately 40% less than that recorded for the two single shot tests. Direct comparison of the PR values alone, would strongly suggest the standard three shot test is much worse than both single shot tests. However, calculation of the CFE gives an accurate account of the flow convergence effects associated with the single shot PR, and doing so confirms an almost identical k_c/k (perforation skin), providing a more accurate representation.

Without further CFD modeling, sole reference to PR values for performance comparison will prove misleading. Results show that any direct comparison between single shot PR values and those involving three charges are not entirely representative. The CFD process enables better quantification of the perforation damage (skin), accounting for boundary and flow convergence effects, allowing each to be compared fairly. Therefore, it becomes relevant to compare the CFE results for test **'P3_13'** to each of the three convergent perforation tests, revealing a range in CFE improvement from 6% to 19% in favour of the convergent perforation geometry models as tested.

Radial Wellbore Performance Modelling

A series of short radial wellbore models were constructed, again using CFD, to better understand the flow performance characteristics for each, matched, perforation geometry model, summarized in table 9:

Table 9—Short Radial Flow Model Description

Model Description	Standard 6 shots/ft; 60° phased	Convergent 2 shots/ft; 90° phased
r_e = 16.4ft (5m) r_w = 0.25ft r_h = 5.00ft Perf = 2.00ft Δp = 870psi k = 100md	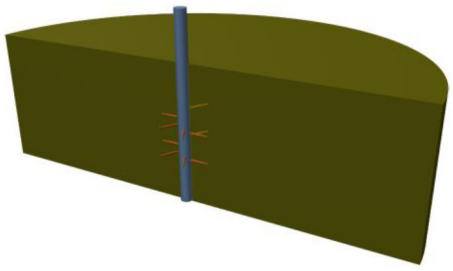	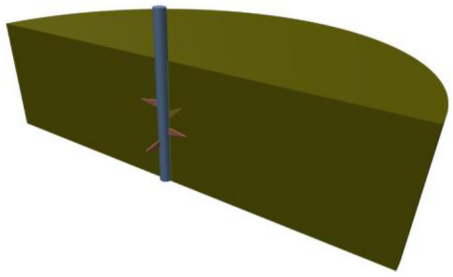

Each radial model made it possible to simulate the corresponding well inflow performance, for a series of realizations, that account directly for perforation phasing and relative shot density variation between the standard and convergent perforation systems.

The simulation models were used to calculate the resulting inflow for each respective perforation geometry over the range of test derived skin (k_c/k) input values. Each radial flow model enabled calculation of the undamaged and damaged inflow. Using the modelled flow output values, and the equation presented below, it is possible to present the corresponding Flow Efficiency [FE], PI and derived well skins for each geometry.

$$FE = \frac{Qd}{Q} = \frac{ln\frac{re}{rw} - 0.75}{\ln\frac{re}{rw} - 0.75 + S}$$

First, we should examine, by direct comparison, the radial inflow performance results for each respective 'matched' Section IV perforation geometry model, as shown in table 10:

Table 10—Matched Section IV Radial Perforation Model Results

Perf. Skin k_c/k [%]	Perforation Geometry Model	Model Results		
		FE	PI	Skin
0.35%	Standard 6 shots/ft; 60° phased	6%	0.015	22.2
0.50%	TriDent 2 shots/ft; 90° phased	7%	0.017	17.9
1.12%	TriStim 2 shots/ft; 90° phased	31%	0.066	3.0

Each radial model can now easily be compared directly to other corresponding laboratory tested perforation results. In direct comparison with the standard 6 shots/ft model, the partially convergent 'TriDent' model is shown to uphold a performance advantage. Given the 'TriDent' geometry was matched to a lesser perforation damage (k_c/k), using the tested lab data, the comparison to the standard model shows the relative 'TriDent' PI is increased by 13%, with an overall well skin reduction of circa. 20%, sufficient to overcome any shot phasing and relative shot density effects.

Comparing the same standard matched model to the fully converged TriStim model, shows PI has been improved by a factor >4.0, reducting skin by >85%. While these results are striking, and may not be directly indicative of actual well potential given the limitations of the test set-up, they are fully reflective of the tested and matched perforation geometries.

In order to understand the direct influence of the perforation geometry on the resulting radial flow performance, a further set of realizations were carried out, using the same perforation skin inputs accross each geometry model. The results are shown in table 11:

Table 11—Radial Model k_c/k Sensitivity Results

Perf. Skin k_c/k [%]	Flow Efficiency [%]			Productivity Index			Total Skin		
	Standard	TriDent	TriStim	Standard	TriDent	TriStim	Standard	TriDent	TriStim
0.35%	6%	5%	11%	0.015	0.012	0.023	22.2	25.5	11.3
0.50%	8%	7%	15%	0.021	0.017	0.031	15.6	17.9	8.0
1.12%	17%	15%	31%	0.044	0.036	0.066	6.7	7.7	3.0

Where equal perforation skin values are modelled for each geometry, the results indicate the emergence of a performance disadvantage with the partially converged 'TriDent' geometry, as compared to the standard perforation model. Whilst the flow efficiency is reduced only by around 1-2% on average, PI is reduced by approx. 20% by comparison, consistently across all k_c/k input values. This reduction in performance is primarily caused by the reduced phasing and relative shot density effect, resulting in an increased total skin of approx. 15%.

The performance increase becomes more apparent where complete convergence, TriStim geometry, is achieved. The TriStim geometry model shows that through a modest increase in relative perforation surface area, as well as a significant increase in tunnel volume, all phasing and relative shot density effects are more than compensated. Again, compared to the standard perforation model, for identical perforation skin values, the results show an average PI increase in favour of the TriStim geometry of circa. 50%, with a similar percentage reduction in total skin evident, showing that optimized geometry can have a significant and positive influence on flow performance.

Conclusions

Despite controlled attempts to achieve good perforation clean-up, through applied DUB. The high skin, or severe apparent k_c/k damage, appears to be a natural consequence of the test set-up. Testing under an axial flow conditions means there is a greater level of flow restriction through the core than would otherwise be the case for a radial set-up. This seemingly inhibits effective perforation clean-up, resulting in higher the skin values as tested for all geometries.

It is suspected that the reduction in effective perforation length is a considerable factor influencing the damage effect. Given it was not possible to properly / accurately determine L_{eff} from the lab tests, crushed damage (k_c) was used as the sole proxy for the test performance matching, proving to be a robust approach.

Comparison to the PR data alone shows an overall consistent improvement of between 30 – 50%, favouring the convergent design. However, appropriate performance comparison must be conducted through CFD analysis.

Matching of the test data, using CFD, highlights consistency with damage required to match the flow data for each geometry model. Mathcing highlighting that for all convergent tests the damage sustained, as a result of perforating, was considerably reduced. Calculated CFE values, for the same matched tests, shows the convergent system outperforms the standard set-up by 6 – 19% overall.

Radial flow models, incorporating the matched perforations, show by direct comparison, the convergent design upholds a flow performance benefit, where shot phasing and relative shot density have been accounted for. Results highlight convergent perforations can improve flow efficiency by up to 25%, with a comparative skin reduction of up to 85%, and a minimum PI improvement of 13%.

Further radial models, using 'like for like' skin inputs (k_c/k) for each perforation geometry, showed the non-ideal TriDent geometry delivered 20% reduction in PI due to phasing and shot arrangement effects. However, where the fully convergent, TriStim geometry, is modelled, PI is shown to increase by circa. 50% over the standard HSD system.

It appears that the main driver for performance enhancement, resulting from the convergent design, is a reduction in overall perforation damage, where phasing and relative shot density effects can be more than compensated through increased perforation channel surface area and improved flow conductivity.

Acknowledgement

The authors would like to thank LR Senergy and DynaEnergetics for their permission to publish this material. Additionally we would like to thank Denis Will (DynaEnergetics) for his support in performing these tests.

Nomenclature

S	= Skin
S_{perf}	= Perforation Skin
k	= permability
k_c	= Crushed Permeability
t_c	= Crushed thickness
mD	= milidarcy
L_{eff}	= effective perforation length
HSD	= High Shot Density
SPF	= Shots per Foot
SUB	= Static Underbalance
DUB	= Dynamic Underbalance
OMS	= Odourless Mineral Spirit
CFE	= Core Flow Efficiency
FE	= Flow Efficiency
PI	= Productivity Index
CFD	= Computational Fluid Dynamics
Δp	= Pressure drop (differential pressure)
r_e	= Reservoir radius
r_w	= Wellbore radius
Q	= Flow rate
Q_d	= Damaged flow rate

References

Byrne, M., Jimenez, M. A., and Chavez, J. C., Senergy, 2009, Predicting Well Inflow Using Computational Fluid Dynamics—Closer to the Truth?, *SPE 122351-MS*

M. T. Byrne, M. A. Jimenez, and E. A. Rojas, Senergy, and J. C. Chavez, GDF Suez, "Modeling Well inflow Potential in Three Dimensions Using Computational Fluid Dynamics", *SPE 128082,* SPE International Symposium and Exhibition on Formation Damage Control, 10-12 February 2010, Lafayette, Louisiana, USA.

Juliane Heiland, Brenden Grove, Jeremy Harvey, Ian Walton, and Andrew Martin, Schlumberger, "New Fundamental Insights into Perforation-Induced Formation Damage", *SPE 122845*

Baoyan Li, Datong Sun, Rajani Satti, SPE, Baker Hughes, "Statistical Analysis of Significant Factors Affecting Perforation Flow at Well Scale", SPE 150122

J. Harvey, P. Kokel, L. Zhan, B. Grove, H. Huang, D. Atwood, SPE, Schlumberger, "Determining Perforation Parameters from Single-Shot Tests: Radial vs. Axial Flow", *SPE 143993*